JOURNAL OF Materials CHEMISTRY

Alkali metal and alkaline earth metal ion exchange with Na-4-mica prepared by a new synthetic route from kaolinite

Tatsuya Kodama†* and Sridhar Komarneni

Materials Research Laboratory and Department of Agronomy, The Pennsylvania State University, University Park, PA 16802, USA. E-mail: tkodama@eng.niigata-u.ac.jp; komarneni@psu.edu

Received 5th January 1999, Accepted 8th June 1999

The ion exchange selectivities of a high-charge-density fluorophlogopite mica, Na-4-mica (ideal chemical composition $Na_4Mg_6Al_4Si_4O_{20}F_4{\cdot}xH_2O$) were investigated for alkali metal ions (Li^+, K^+ and Cs^+) and alkaline earth metal ions (Sr^{2+} and Ba^{2+}). The ion exchange isotherms were obtained at room temperature using Na-4-mica with a hydrated 12.11 Å lattice, which was easily and economically prepared from a mixture of NaF, MgO and calcined kaolinite. The selectivity depended considerably on the degree of loading of metal ions in the mica for the alkaline earth metals, but not for the alkali metal ions. The selectivity increased in the order: $Li^+ < Cs^+ < K^+ < Na^+$ for alkali metal and $Sr^{2+} < Ba^{2+}$ for alkaline earth metal ions. Mg^{2+}-exchanged Na-4-mica with an expanded 13.33 Å lattice was also prepared and its strontium and barium ion exchange were studied.

Introduction

Mica is one of the most representative of the 2 : 1 phyllosilicates, *i.e.* each layer consists of an octahedral sheet sandwiched between two tetrahedral sheets. Micas are distinguished from smectites or vermiculites by their higher layer charge density. The two main categories of micas based on layer charge density are: 1) true micas with 1 negative charge per formula unit, and 2) brittle micas with 2 negative charges per formula unit. Owing to the high charge density, naturally occurring micas do not normally swell in water and other polar solvents, and as a result exchange reactions with the interlayer cations do not readily occur. Thus, studies on the ion exchange of clay minerals were for many years restricted to low-charge-density materials, such as the smectite and kaolinite types, and their synthetic analogues, *e.g.* laponite.[1,2] These phyllosilicates typically have ion exchange capacities of less than 100 milli-equivalents (mequiv) per 100 g of dry clay. Synthetic micas with ion exchange capacities of 200 to 250 mequiv $(100\ g)^{-1}$ have been recently prepared and these are of considerable interest.[3–5] However, all the synthetic swelling micas prepared to date are of the true mica type except for one which is of the brittle mica type and was named Na-4-mica.[6–12]

Na-4-mica, a very highly charged sodium fluorophlogopite mica of theoretical chemical composition $Na_4Mg_6Al_4Si_4O_{20}F_4{\cdot}xH_2O$, was first prepared by Gregorkiewitz *et al.* in 1974.[6] Na-4-mica has a theoretical ion-exchange capacity of 468 mequiv $(100\ g)^{-1}$ on an anhydrous basis. Although Na-4-mica is a very highly charged phyllosilicate of the brittle mica-type, it has the unique advantage of becoming hydrated on contact with water or even in moist air at ambient conditions.[6–12] Na-4-mica contains an unusually large number of 4 interlayer cations per unit cell. No mica with more than 2 interlayer cations per unit cell had ever been observed before. The presence of this unusually large number of interlayer cations, and the resulting offset layer stacking by 1/3 *′b′*, allows the structure to expand from a dehydrated 9.81 Å to a hydrated 12.18 Å *c*-axis spacing to achieve a more thermodynamically stable interlayer structure.

Gregorkiewitz *et al.* synthesized flakes of Na-4-mica (0.1–2 mm), but only in small quantities with large amounts of impure phases.[7] One of the present authors previously reported that a very fine and pure phase of Na-4-mica, which is essential for practical applications, could be prepared by a solution-sol–gel process using tetraethoxysilane, aluminium and magnesium nitrates.[8] Preliminary cation exchange experiments based on measurements of the distribution coefficients (K_d) were reported on the solution-sol–gel processed Na-4-mica, showing that the Na-4-mica has high ion-exchange selectivities for many divalent transition metal ions and for strontium and barium, but not for the alkali metal ions, magnesium and calcium from 0.5 N NaCl.[9] The sol–gel synthetic method, however, is not cost-effective because of the use of expensive chemicals such as tetraethoxysilane and the long and complicated procedure. However, a somewhat simplified procedure was later developed for the synthesis of this mica using fumed silica as the silica source.[10] For waste disposal or metal recovery applications, it was necessary to develop an even more cost-effective synthetic process for Na-4-mica.

Recently, we have found an easy and economical synthetic process for Na-4-mica using calcined kaolinite (metakaolin) as a very cheap aluminosilicate source with the desired 1 : 1 Si to Al molar ratio.[11] With the Na-4-mica prepared from metakaolin, detailed thermodynamic studies using Kielland plots (plot of the corrected selectivity coefficient K_{Na}^{M} *vs.* fractional exchange, $\overline{X}_M$) were carried out on $2Na^+ \rightarrow M^{2+}$ exchange for the divalent transition metals Cd, Ni, Co, Mn and Zn.[12] Na-4-mica has high cation-exchange capacities for the above ions, ranging from 187 to 195 mequiv $(100\ g)^{-1}$, and the sequence of the selectivity was found to be $Zn^{2+} > Ni^{2+} \approx Co^{2+} \approx Cd^{2+} > Mn^{2+}$. In the present work, the ion exchange selectivities of the easily and economically synthesized Na-4-mica were investigated for alkali metal ions (Li^+, K^+ and Cs^+) and alkaline earth metal ions (Sr^{2+} and Ba^{2+}) using the distribution coefficient K_d and Kielland plots. Mg^{2+}-exchanged Na-4-mica, which had expanded basal spacings of 13.33 Å, was also prepared and its strontium and barium cation exchange selectivities were studied in comparison to the original Na-4-mica saturated with Na.

†Permanent address: Department of Chemistry & Chemical Engineering, Faculty of Engineering, Niigata University, 8050 Ikarashi 2-nocho, Niigata 950-2181, Japan.

Experimental

Preparation of Na-4-micas from metakaolin

Naturally occurring kaolinite has the desired 1 : 1 Si to Al molar ratio in its chemical composition, $Al_2Si_2O_5(OH)_4{\cdot}xH_2O$ and serves as a good aluminosilicate source for the synthesis of Na-4-mica. A poorly crystallized kaolinite (supplied by Georgia Kaolin Company), ultrafine MgO (supplied by Ube Industries, Ube, Japan) and NaF were the starting materials for the synthesis of Na-4-mica in the present work. The poorly crystallized kaolinite [$Al_2Si_2O_5(OH)_4{\cdot}0.08H_2O$] was first calcined at 700 °C for 18 h to transform it to an amorphous phase (on heating to around 600 °C, kaolinite is completely dehydrated and loses its crystalline character) which is the so-called metakaolin ($Al_2Si_2O_7$). The metakaolin product was cooled and stored in a desiccator over silica gel at room temperature. The water contents of the metakaolin and ultrafine MgO were determined by thermal analysis using a TG DTA 2010, Mac Science instrument. Appropriate proportions of ultrafine MgO and metakaolin were mixed to obtain a stoichiometric composition, which when reduced to pure oxides was exactly $3MgO–Al_2O_3–2SiO_2$. The mixture was combined with an equal mass of NaF and transferred to a platinum vessel. It was heated for 6 h at 890 °C in an air atmosphere furnace. The resulting solid was ground up and washed in deionized water several times to remove the remaining NaF. The remaining low percentage of water-insoluble impure phases, which may include insoluble fluoride salts, were then removed by repeated washings with a saturated boric acid solution. Then, the solid was washed with 1 M NaCl solution three times to completely saturate all the exchange sites with Na^+. The product was again washed with deionized water and dried at 60 °C in an oven for 2–3 days. The Na-4-mica thus prepared was finally stored in a desiccator over silica gel at room temperature. Although as-synthesized Na-4-mica was anhydrous, the washed sample hydrated readily.

Powder X-ray diffraction (XRD) was carried out to check for phase purity, to determine the basal spacings of the Na-4-mica, and to monitor crystallinity using a Rigaku RAD-rA diffractometer with Cu-Kα radiation. Scanning electron microscopy (SEM) was used to determine particle size and shape. An ISI-DS 130 instrument was used for SEM. Water contents of the hydrated Na-4-mica were determined by thermal analysis to be $Na_4Mg_6Al_4Si_4O_{20}F_4{\cdot}2.1H_2O$ (4.24 wt%). Sodium, magnesium, aluminium, silicon, iron and titanium contents were determined by lithium borate fusion and chemical analyses by atomic emission spectrometry (SpectraSpan III instrument) for hydrated Na-4-mica (Table 1). Fluoride was determined by ion-selective electrode analysis. The chemical composition from the chemical analyses ($Na_{3.14}Mg_{5.41}Ti_{0.05}Al_{4.07}Fe_{0.01}Si_4O_{19.3}F_{3.83}$) was almost consistent with the ideal composition.

Preparation of Mg^{2+}-exchanged Na-4-mica

Mg^{2+}-exchanged Na-4-mica was obtained by treatment of Na-4-mica with a 1 M solution of magnesium nitrate at 60 °C for 3 days. The solution was renewed daily. The product was washed with deionized water and dried at 60 °C in an oven for 2–3 days. It was finally stored in a desiccator over silica gel at room temperature. Water contents of hydrated Na-4-mica were determined by thermal analysis. Powder X-ray diffraction (XRD) was carried out to check for phase purity, to determine the basal spacings, and to monitor crystallinity.

Table 1 Analytical data for the hydrated Na-4-mica

Content (wt%)							
SiO_2	Al_2O_3	TiO_2	Fe_2O_3	MgO	Na_2O	F	H_2O
26.1	22.6	1.24	0.68	23.6	10.6	7.9	4.24

Cation exchange isotherm determination

A 25 mg portion of Na-4-mica (anhydrous basis) was equilibrated with 25 cm^3 of a mixed solution having different mole ratios of Na^+/M^{n+} ($M^{n+}=Li^+$, K^+, Cs^+, Sr^{2+} or Ba^{2+}) with shaking at 25 °C for 4 weeks (as mentioned later, in the kinetic study of Na^+/Sr^{2+} exchange with Na-4-mica, it took 4 weeks for the Sr^{2+} exchange reaction to complete. This is because Na-4-mica has a high layer charge and narrow interlayer basal spacing of about 12 Å). The total normality of the solutions was kept constant at 0.00468 N except for two solutions containing only M^{n+} (K^+, Sr^{2+} and Ba^{2+}) without Na^+ for which total normalities of 0.00585 and 0.00702 N were used. After equilibration, the supernatant solution was analyzed for alkali metal and alkaline earth metal ions by atomic emission spectroscopy. The amounts of metal ions exchanged or released by Na-4-mica were determined from the difference in the concentration between the sample solution and the reference. All these equilibrium studies were conducted in triplicate to check for reproducibility. The errors in these repeated experiments were about ±5%. The theoretical cation-exchange capacity [468 mequiv $(100\ g)^{-1}$ of the anhydrous form] was used for representing the ion exchange isotherms.

The ion exchange isotherm for $Mg^{2+}\rightarrow Sr^{2+}$ exchange in Mg^{2+}-exchanged Na-4-mica was obtained in a similar way. A 25 mg portion of Mg^{2+}-exchanged Na-4-mica (anhydrous form) was equilibrated with 25 cm^3 of a mixed solution having different mole ratios of Mg^{2+}/Sr^{2+} or Mg^{2+}/Ba^{2+} with shaking at 25 °C for 4 weeks.

Strontium uptake kinetics study

Strontium uptake kinetics were determined on Na-4-mica and Mg^{2+}-exchanged mica by equilibrating 20 mg of sample with 25 cm^3 of 0.5 M NaCl containing 0.0001 M $SrCl_2$ for different periods in a batch experiment. Three repeated experiments were performed for each duration. After equilibration, the solid and solution phases were separated by a filter syringe (for 1, 2, 5 and 30 min) or by centrifugation (for 2 h, 8 h, 1 day, 1 week and 4 weeks). The solutions were analyzed for Sr^{2+} remaining in solution by atomic emission spectroscopy.

Theoretical

The cation exchange process between Na^+ and M^{n+} on Na-4-mica is represented by

$$n\overline{Na}^+ + M^{n+} \rightleftharpoons nNa^+ + \overline{M}^{n+} \quad (1)$$

where the bar above the symbols represents the ion-exchanger phase. The thermodynamic equilibrium constant, K, of the reversible ion-exchange reaction is defined by

$$K = \frac{[Na^+]^n \overline{X}_M \gamma^n_{Na} f_M}{[M^{n+}]\overline{X}^n_{Na}\gamma_M . f^n_{Na}} \quad (2)$$

where $[Na^+]$ and $[M^{n+}]$ are the molalities of the ions in solution, γ_i and f_i are activity coefficients in the solution phase and in the ion-exchanger phase, respectively. The standard states are taken for the ion-exchanger phase as the exchanger is in its pure Na^+ form and pure M^{n+} form, and the activity coefficients, f_{Na} and f_M, are set at unity when the exchanger is at the standard state of the Na^+ form and the M^{n+} form, respectively. γ_{Na} and γ_M are unity when $[Na^+]$ and $[M^{n+}]$

approach zero. $\overline{X}_i$ is an equivalent fraction of ion i in the ion-exchanger phase, defined by

$$\overline{X}_{Na} = \frac{[\overline{Na}^+]}{n[\overline{M}^{n+}] + [\overline{Na}^+]}, \overline{X}_M = \frac{n[\overline{M}^{n+}]}{n[\overline{M}^{n+}] + [\overline{Na}^+]} \quad (3)$$

$$[\overline{Na}^+] + n[\overline{M}^{n+}] = TC \quad (4)$$

where TC represents the theoretical or total capacity.

The molalities $[Na^+]$ and $[M^{n+}]$ can be replaced by the equivalent fractions of the ions in the solution (X_i):

$$X_{Na} = \frac{[Na^+]}{n[M^{n+}] + [Na^+]}, X_M = \frac{n[M^{n+}]}{n[M^{n+}] + [Na^+]} \quad (5)$$

$$[Na^+] + n[M^{n+}] = TN \quad (6)$$

where TN represents the total normality of the solution. Using a corrected selectivity coefficient, K^M_{Na}, the thermodynamic equilibrium constant is rewritten as[13]

$$K = K^M_{Na} \frac{f_M}{f^n_{Na}} \quad (7)$$

where

$$K^M_{Na} = \frac{X^n_{Na}\overline{X}_M\gamma^n_{Na}}{X_M\overline{X}^n_{Na}\gamma_M}[n(TN)^{n-1}] = \frac{(1-X_M)^n\overline{X}_M\gamma^n_{Na}}{X_M(1-\overline{X}_M)^n\gamma_M}[n(TN)^{n-1}] \quad (8)$$

As shown by eqn. (8), the corrected selectivity coefficient is dependent on the total normality. The ratio of the activity coefficients γ^n_{Na}/γ_M can be calculated by using $\gamma_{\pm NaY}$ and $\gamma_{\pm MYn}$, where Y denotes the common anion, according to Glueckauf's relation.[14] A corrected selectivity coefficient larger than unity ($\ln K^M_{Na} > 0$) indicates selectivity for the ion M^{n+}.[15] Na^+ ions are more preferred if K^M_{Na} is smaller than unity ($\ln K^M_{Na} < 0$). When K^M_{Na} is equal to unity ($\ln K^M_{Na} = 0$), no preference between these ions is indicated.

If the Gibbs–Duhem equation is applied to the ion-exchange reaction, the thermodynamic equilibrium constant, K, is given by the integration of the Kielland plot from $\overline{X}_M = 0$ to $\overline{X}_M = 1$.[16–18]

$$\ln K = (1-n) + \int_0^1 \ln K^M_{Na} d\overline{X}_M + \Delta \quad (9)$$

The third term on the right, Δ, is negligible when compared with experimental accuracy in measuring the equilibrium.[13] A plot of $\log K^M_{Na}$ *vs.* $\overline{X}_M$ (Kielland plot) is generally represented by the polynomial function.[19]

$$\log K^M_{Na} = \sum_{m=1} (m+1) C_m \overline{X}^m_M + \log(K^M_{Na})_{X_M, \overline{X}_M \to 0} \quad (10)$$

where the coefficient, C_m, is the generalized Kielland coefficient.

Eqn. (9) and (10) are combined to give the thermodynamic constant K.

$$\ln K = (1-n) + 2.303 \sum_m C_m + \ln(K^M_{Na})_{X_M, \overline{X}_M \to 0} \quad (11)$$

Thus, the thermodynamic equilibrium constant is determined by the valences of the exchanging cation (n), the generalized Kielland coefficients (C_m) and the intercept of the Kielland plot, $(K^M_{Na})_{X_M, \overline{X}_M \to 0}$. The Kielland plots often give linear relationships with a slope of $2C_1$, in which case eqn. (10) can become

$$\log K^M_{Na} = 2C_1\overline{X}_M + \log(K^M_{Na})_{X_M, \overline{X}_M \to 0} \quad (12)$$

The generalized Kielland coefficient, C_1, is related to the energy term for the steric limitation or jumping barrier for the exchanging ions in the interlayer.[20] Generally, C_1 is a negative constant value depending on the ion exchanger system. This means that ion exchange becomes more difficult with progressive exchange. In this case, the energy term for the steric limitation increases as the $|C_1|$ value increases.

The Gibbs standard free energy change ΔG° can be calculated by

$$\Delta G^\circ = -RT \ln K \quad (13)$$

The K_d value at infinitesimal exchange (very small $\overline{X}_M$) is very important for interpreting the chromatographic behavior of metal ions. It is defined by

$$K_d = \frac{[\overline{M}^{n+}]}{[M^{n+}]} \quad (14)$$

Using eqn. (3)–(6), we obtain

$$K_d = \frac{TC\overline{X}_M}{TNX_M} \quad (15)$$

The cation exchange reaction between Mg^{2+} and M^{2+} on Mg^{2+}-exchanged Na-4-mica is represented by

$$\overline{Mg}^{2+} + M^{2+} \rightleftarrows Mg^{2+} + \overline{M}^{2+} \quad (16)$$

The thermodynamic equilibrium constant, K, is defined by

$$K = \frac{[Mg^{2+}]\overline{X}_M\gamma_{Mg}f_M}{[M^{2+}]\overline{X}_{Mg}\gamma_M f_{Mg}} \quad (17)$$

Thus, these equations for the $nNa^+ \rightarrow M^{n+}$ exchange reaction in the case of $n=1$ can be applied to this $Mg^{2+} \rightarrow M^{2+}$ exchange reaction.

Results and discussion

Preparation of Na-4-mica and Mg^{2+}-exchanged mica

Fig. 1a shows the XRD pattern of Na-4-mica prepared from a mixture of NaF, ultrafine MgO, and metakaolin as the aluminosilicate source. That Na-4-mica was synthesized is evident from the presence of the first order (001) reflection in the XRD pattern. The very strong peak observed at $d = 12.11$ Å

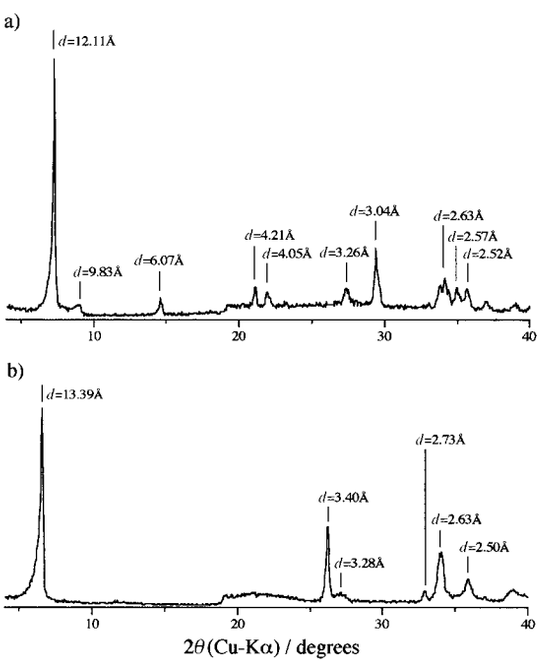

Fig. 1 XRD patterns of a) Na-4-mica prepared by crystallization at 890 °C for 6 h from a mixture of NaF, ultrafine MgO and metakaolin, and b) Mg^{2+}-exchanged Na-4-mica.

corresponds to the basal spacing for the hydrated form of Na-4-mica with a single sheet of interlayer water.[7] Strong peaks observed at $d=6.07$, 4.05 and 3.04 Å can be assigned to the (002), (003) and (004) reflections of the c-axis spacing of the hydrated form. The peak observed at $d=9.83$ Å was attributed to the basal spacing of the anhydrous form. The peak at $d=3.26$ Å is characteristic of the anhydrous form, and can be assigned to the (003) and (022) reflections. Scanning electron microscopy revealed pseudo-hexagonal crystallites. The Na-4-mica had a large particle-size distribution, ranging from 0.5 to 5 μm. Many crystallites were larger than 2.5 μm.

Fig. 1b shows the XRD pattern of Mg^{2+}-exchanged Na-4-mica. The strong peak for the (001) reflection of hydrated Na-4-mica was shifted to $d=13.39$ Å. This is due to the formation of a structure containing double sheets of interlayer water. A layer spacing of 13.82 Å has been reported for magnesium vermiculite prepared by progressive removal of interlayer water from the normal magnesium vermiculite ($d_{001}=14.36$ Å) with double sheets of interlayer water.[21] Upon dehydration of the normal 14.36 Å phase, a 13.82 Å phase is first formed corresponding to a structure containing double sheets of interlayer water with an arrangement different from that in the 14.36 Å phase. A similar structure with double sheets of interlayer water was apparently formed in Mg^{2+}-exchanged Na-4-mica. The water content of the mica increased from 4.24 to 11.82 wt% after the Mg^{2+}-exchange treatment. This phase has about six H_2O molecules per unit cell. The peaks for the (002) and (003) reflections disappeared and a strong peak appeared at $d=3.40$ Å, which is due to the (004) reflection. Similar XRD patterns are observed for Co^{2+}- and Ni^{2+}-exchanged Na-4-micas, in which strong XRD peaks for the (00l) reflections appear only at $d=13.5$ and 3.4 Å in the 2θ range 4–30° (Cu-Kα radiation). The reason why the peaks for the (002) and (003) reflections disappear for Mg^{2+}-, Co^{2+}- and Ni^{2+}-exchanged micas is not clear.

Ion exchange properties of Na-4-mica

The isotherms for $Na^+ \rightarrow Li^+$, K^+, and Cs^+ exchange with Na-4-mica are plotted in Fig. 2a as the equivalent fraction of the cation in the Na-4-mica phase against the equivalent cation fraction in the solution. The K^+ and Cs^+ exchange isotherms appeared to be sigmoid-type curves, which are often observed in the ion exchange isotherms of inorganic ion-exchange materials.[22,23] The differences in the concentrations of Li^+ between the equilibrated sample solutions and the references were very minor and did not fall outside the experimental errors for chemical analysis, indicating no selectivity for Li^+. Since we could not accurately determine the $[\overline{Li^+}]$ taken up because the values were too low, we assumed $\overline{X}_{Li}=0$ for the isotherm in Fig. 2a. In the case of cation exchange between cations with the same valence (*e.g.* monovalent–monovalent exchange, divalent–divalent exchange), the diagonal line in the isotherm indicates the non-preference isotherm.[24] M^+ ions are preferred over Na^+ if the plots fall above the diagonal line ($K^M_{Na}>1$), while Na^+ ions are preferred if the plots fall below the diagonal line ($K^M_{Na}<1$). As indicated by the isotherms with respect to the diagonal line, the selectivity increased in the order of $Li^+<Cs^+<K^+<Na^+$. The isotherms for $2Na^+ \rightarrow Sr^{2+}$ and Ba^{2+} exchanges were different from those for Li^+, K^+ and Cs^+ exchange (Fig. 2b). The isotherms quickly increased and flattened out. The cation exchange appeared to be limited at $\overline{X}_{Sr}<0.12$ and $\overline{X}_{Ba}<0.25$ for $2Na^+ \rightarrow Sr^{2+}$ and Ba^{2+} exchange, respectively. From the isotherms, the selectivity order was $Sr^{2+}<Ba^{2+}$ and the cation exchange capacities (CECs) for Sr^{2+} and Ba^{2+} were determined to be 56 and 117 mequiv $(100\ g)^{-1}$, respectively.

Fig. 3 shows the Kielland plots for the cation exchange reactions. Plots for $Na^+ \rightarrow Li^+$ exchange were not obtained because we could not accurately determine $\overline{X}_{Li}$ and then K^{Li}_{Na}. For cation exchange with alkali metal ions, the corrected selectivity coefficient K^M_{Na} did not change dramatically for the equivalent fraction of the cation in the mica, $\overline{X}_M/K^K_{Na}$ values were of the order of 10^{-1}–1.0 and K^{Cs}_{Na} values of the order of 10^{-2}–10^{-1} for $\overline{X}_M$. For alkaline earth metal ions, however, the corrected selectivity coefficient quickly and drastically decreased when $\overline{X}_M$ increased. The K^{Sr}_{Na} value decreased from of the order of 10^{-1} to 10^{-4} and the K^{Ba}_{Na} value from 10 to 10^{-4} for increasing $\overline{X}_M$. We could not calculate ΔG° values for these cation exchange reactions because the Kielland plots were obtained only in small regions as shown in Fig. 3: ΔG° is obtained from the integration of a Kielland plot from $\overline{X}_M=0$ to $\overline{X}_M=1$.

In the present work, Sr^{2+} and Ba^{2+} exchange reactions can not proceed beyond $\overline{X}_{Sr}=0.12$ and $\overline{X}_{Ba}=0.25$. One of the present authors previously reported $2Na^+ \rightarrow Sr^{2+}$ exchange with solution-sol–gel processed Na-4-mica with crystallite sizes <1 μm.[8] The solution-sol–gel processed Na-4-mica was reported to have 216 mequiv $(100\ g)^{-1}$ of strontium exchange capacity, which is much larger than that for Na-4-mica prepared from metakaolin in the present work. In the strontium exchange, the isotherm flattened out at $\overline{X}_{Sr}=0.4$. The interlayer spacing collapsed considerably when about half of the exchange sites were occupied by strontium, as confirmed by powder X-ray diffraction which showed that the c-axis decreased from 12.2 to 10.2 Å and that the peak for the (001) reflection became very weak and broadened. This collapse was considered to determine the limitation of $\overline{X}_{Sr}$ for the solution-sol–gel processed Na-4-mica. In the present work, the (001) reflection peak for the hydrated phase remained strong and that for the anhydrous phase was not detected in the XRD

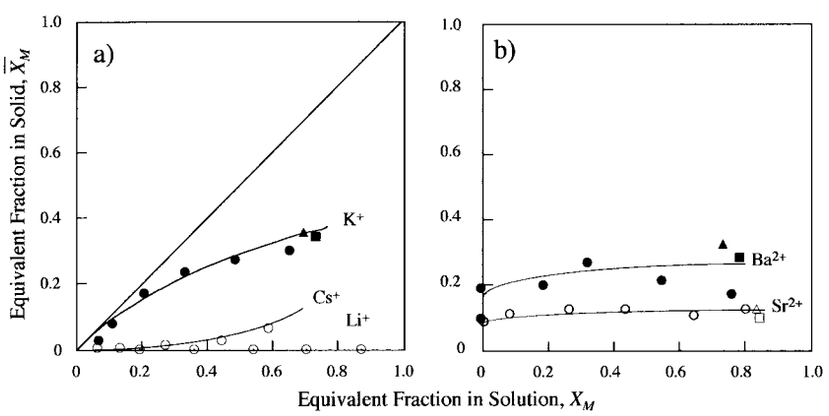

Fig. 2 Cation exchange isotherms with Na-4-mica at room temperature. a) $Na^+ \rightarrow Li^+$ (⊙), K^+(●, ▲, ■) and Cs^+(○) exchange isotherms. b) $2Na^+ \rightarrow Sr^{2+}$ (○, △, □) and Ba^{2+}(●, ▲, ■) exchange isotherms. Total normalities used were 0.00468 N (circles), 0.00585 N (triangles), and 0.00702 N (squares).

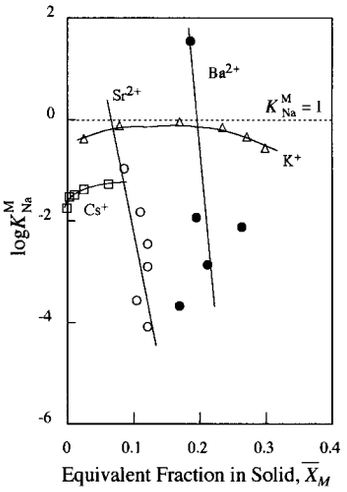

Fig. 3 Kielland plots for $Na^+ \rightarrow K^+$ (△) and Cs^+ (□) exchange, and $2Na^+ \rightarrow Sr^{2+}$ (○) and Ba^{2+} (●) exchange on Na-4-mica. Total normality used was 0.00468 N.

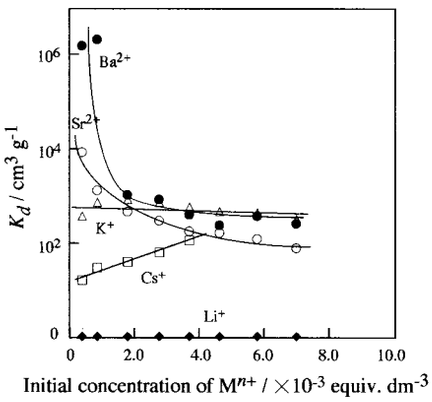

Fig. 4 Change in distribution coefficient (K_d) as a function of initial concentration of M^{n+}. $Na^+ \rightarrow Li^+$ (◆), K^+ (△) and Cs^+ (□) exchange and $2Na^+ \rightarrow Sr^{2+}$ (○) and Ba^{2+} (●) exchange.

patterns of Sr^{2+}-exchanged Na-4-micas. But a very weak and broadened peak was observed at $d = 3.26$ Å, which is a characteristic XRD peak for the anhydrous phase. In the XRD patterns of Ba^{2+}-exchanged Na-4-mica, small peaks for the anhydrous phase were clearly observed at $d = 9.77$–9.83 Å and $d = 3.26$ Å along with strong peaks for the hydrated phase. Thus, there is the possibility that the collapse of the interlayer spacing was caused by Sr^{2+} or Ba^{2+} exchange only at the edges of the large crystals in the Na-4-mica prepared from metakaolin, which prevents the exchange reaction from proceeding to the interior of the crystal. However, since the original Na-4-mica had contained a very small amount of anhydrous phase (Fig. 1a), we could not corroborate that the formation of this small amount of anhydrous phase was caused by Sr^{2+} or Ba^{2+} exchange in the present work. Further investigation of the Sr^{2+} or Ba^{2+} exchange reaction in Na-4-mica is needed in order to clarify the reasons why an $\overline{X}_M$ limit exists for strontium and barium exchange and why the strontium exchange capacities are very different between these differently synthesized Na-4-micas.

The distribution coefficients (K_d) were calculated using eqn. (15), and are plotted against the initial concentration of M^{n+} in the solution in Fig. 4. For low concentrations of M^{n+}, K_d values were of the order of 10^4 and 10^6 for Sr^{2+} and Ba^{2+}, respectively, which were much higher than those for K^+, Cs^+ and Li^+. The K_d values for Sr^{2+} and Ba^{2+} decreased considerably when the initial concentration of M^{n+} was increased, while those for the alkali metal ions did not change so drastically. The considerable decrease in the K_d values of Sr^{2+} and Ba^{2+} comes from the $\overline{X}_{Sr}$ and $\overline{X}_{Ba}$ limits. Na-4-mica is effective for the separation of Sr^{2+} and Ba^{2+} when the loading of cations in the mica is low ($\overline{X}_{Sr} < 0.12$ and $\overline{X}_{Ba} < 0.25$).

Strontium and barium exchange properties of Mg^{2+}-exchanged Na-4-mica

The interlayer spacing is expanded from 12.11 to 13.39 Å in Mg^{2+}-exchanged Na-4-mica (Mg-form). This hydrated phase was used for strontium and barium exchange. The strontium and barium exchange isotherms were obtained in Mg^{2+}/Sr^{2+} or Mg^{2+}/Ba^{2+} solutions, assuming $Mg^{2+} \rightarrow Sr^{2+}$ or Ba^{2+} exchange in the Mg-form (Fig. 5a). The strontium and barium isotherms fell below those for $2Na^+ \rightarrow Sr^{2+}$ or Ba^{2+} exchange (Fig. 2b) in the original Na-4-mica (Na-form). $Mg^{2+} \rightarrow Sr^{2+}$ or Ba^{2+} exchange in the Mg-form was less selective in comparison to $2Na^+ \rightarrow Sr^{2+}$ or Ba^{2+} exchange in the Na-form. In the Kielland plots (Fig. 5b), K^{M}_{Mg} decreased considerably with increasing $\overline{X}_M$, like the Kielland plots for $2Na^+ \rightarrow Sr^{2+}$ or Ba^{2+} exchange in the Na-form (Fig. 3).

The kinetics of Sr uptake is an important aspect in any practical application, *e.g.* radioactive Sr separation from nuclear waste solutions. Fig. 6 shows the Sr exchange kinetics of the Na-form and the Mg-form. Only 37% of the added Sr was taken up over 24 h by the Na-form. Selective Sr uptake from a 0.5 M NaCl background solution was almost complete after 4 weeks (674 h): the uptake was more than 96%. Sr uptake

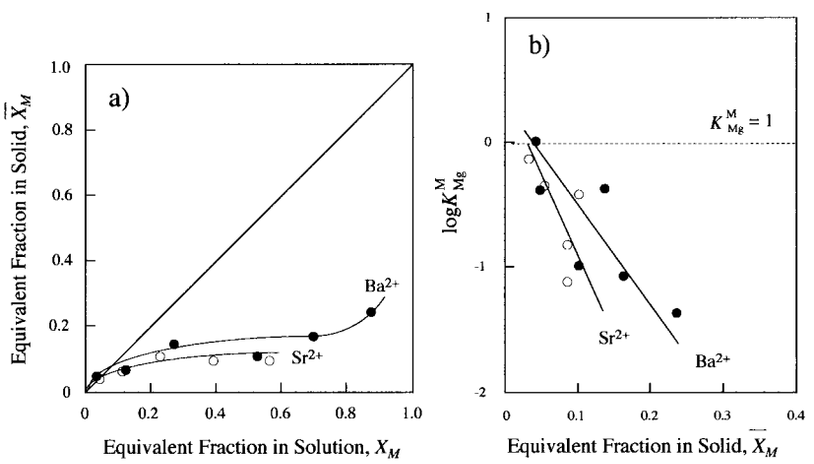

Fig. 5 Cation exchange isotherms (a) and Kielland plots (b) for $Mg^{2+} \rightarrow Sr^{2+}$ (○) and Ba^{2+} (●) exchange with Mg^{2+}-exchanged Na-4-mica at room temperature. A total normality of 0.00468 N was used.

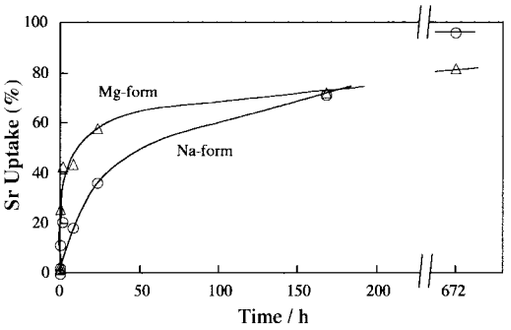

Fig. 6 Sr uptake kinetics by Na-4-mica (Na-form: ○) and Mg^{2+}-exchanged Na-4-mica (Mg-form: △) from 0.5 M NaCl containing 0.0001 M $SrCl_2$.

kinetics were improved by expansion of the interlayer region of the Mg-form in the initial stage of the exchange. About 60% of the added Sr was taken up in 24 h with the Mg-form. However, selective Sr uptake was only 82% even after 4 weeks. The Mg-form showed higher kinetic selectivity but less equilibrium selectivity for strontium in comparison to the Na-form.

Conclusions

For alkali metal ions, the selectivity did not drastically change with the equivalent fraction of the cation in the mica, $\overline{X}_M$. The selectivity increased in the order: $Li^+ < Cs^+ < K^+ < Na^+$. Except for Li^+, the order may be explained by the effective ionic radii (EIR) of the cations: the selectivity for the alkali metal ion increases as the EIR decreases. For the Li^+ ion, it appeared that the cation exchange reaction did not proceed. Li^+ ions have difficulty displacing the Na^+ ions in the interlayer spacings of the mica because of the strong hydration or the large hydrated radius of the Li^+ ion. For the alkaline earth metal ions, Sr^{2+} and Ba^{2+}, the selectivity drastically decreased with increasing $\overline{X}_M$. The cation exchange appeared to be limited at $\overline{X}_{Sr} < 0.12$ and $\overline{X}_{Ba} < 0.25$. The selectivity increased in the order: $Sr^{2+} < Ba^{2+}$.

$Mg^{2+} \rightarrow Sr^{2+}$ or Ba^{2+} exchange in Mg^{2+}-exchanged Na-4-mica was less selective in comparison to $2Na^+ \rightarrow Sr^{2+}$ or Ba^{2+} exchange in the original (Na-saturated) Na-4-mica. However, Sr uptake kinetics or kinetic selectivity for strontium were improved by expansion of the interlayer region.

Acknowledgements

This work was supported by the Interfacial, Transport and Separation Program, Chemical and Transport Systems, Division of the National Science Foundation under Grant No. CTS-9612714.

References

1 H. van Olphen, *An Introduction to Clay Colloid Chemistry*, 2nd edn., Wiley, New York, 1977.
2 B. K. G. Theng, *The Chemistry of Clay Organic Reactions*, Wiley, New York, 1974.
3 Y. Morikawa, T. Goto, Y. Mora-Oka and T. Ikawa, *Chem. Lett.*, 1982, 1667.
4 H. Sakurai, K. Urabe and Y. Izumi, *J. Chem. Soc., Chem. Commun.*, 1988, 1519.
5 J. W. Johnson, J. F. Brody, R. M. Alexander, L. N. Yacullo and C. F. Klein, *Chem. Mater.*, 1993, **5**, 36.
6 M. Gregorkiewitz, J. F. Alcover, J. A. Rausell-Colom and J. M. Serratosa, *2ème Reunion des Groupes Europeens d'Argiles,* Strasbourg, 1974, p. 64.
7 M. Gregorkiewitz and J. A. Rausell-Colom, *Am. Mineral.*, 1987, **72**, 515.
8 W. J. Paulus, S. Komarneni and R. Roy, *Nature* (*London*), 1992, **357**, 571.
9 S. Komarneni, W. J. Paulus and R. Roy, *New Development in Ion Exchange; Proc. Int. Conf. Ion Exchange*, ed. M. Abe, T. Kataoka and T. Suzuki, Kodansha, Tokyo, Japan, 1991, p. 51.
10 K. R. Franklin and E. Lee, *J. Mater. Chem.*, 1996, **6**, 109.
11 S. Komarneni, R. Pidugu and J. E. Amonette, *J. Mater. Chem.*, 1998, **8**, 205.
12 T. Kodama and S. Komarneni, *J. Mater. Chem.*, 1999, **9**, 533.
13 R. M. Barrer and J. Klinowski, *J. Chem. Soc., Faraday Trans. 1*, 1974, **70**, 2080.
14 E. Glueckauf, *Nature*, 1949, **163**, 414.
15 F. Helfferich, *Ion Exchange*, Daver, New York, 1995, p. 170.
16 J. Kielland, *J. Soc. Chem. Ind.*, 1935, **54**, 232T.
17 E. Ekedahl, E. Högfeldt and L. G. Sillén, *Acta Chem. Scand.*, 1950, **4**, 556.
18 G. L. Gaines Jr. and H. C. Thomas, *J. Chem. Phys.*, 1953, **21**, 714.
19 R. M. Barrer, *Natural Zeolites, Occurrence, Properities, Use*, ed. L. B. Sand and F. A. Mumpton, Pergamon, New York, 1978, p. 385.
20 R. M. Barrer and J. D. Falconer, *Proc. R. Soc. London A*, 1956, **236**, 227.
21 R. E. Grim, *Clay Mineralogy*, 2nd edn., McGraw-Hill, New York, 1968, p. 104.
22 M. Abe, *J. Inorg. Nucl. Chem.*, 1979, **41**, 85.
23 M. Abe, K. Yoshigasaki and T. Sugiura, *J. Inorg. Nucl. Chem.*, 1980, **42**, 1753.
24 M. Tsuji and S. Komarneni, *J. Mater. Res.*, 1989, **4**, 698.

Paper 9/00113A